Resonance electron scattering from adsorbed molecules: Angular distribution of inelastically scattered electrons and application to physisorbed O_2 on graphite

P. J. Rous, R. E. Palmer, and R. F. Willis
The Cavendish Laboratory, University of Cambridge, Madingley Road, Cambridge CB3 0HE, United Kingdom
(Received 9 March 1988; revised manuscript received 2 December 1988)

We present a theoretical study of the angular distribution of electrons inelastically scattered after the vibrational excitation of molecules adsorbed upon crystalline surfaces through the formation of temporary negative ions. We develop a theoretical framework by which these angular emission profiles may be calculated and interpret measured angular distributions from a negative-ion resonance near 9 eV in physisorbed O_2 on graphite. Using this method, we determine both the resonance symmetry and the orientation of the O_2-molecular axis within the overlayer. The theory employs a proper treatment of the multiple scattering of the incident and emitted electrons within the surface which we show to be important in the energy range within which resonances are commonly observed.

I. INTRODUCTION

Recently we reported[1] the first observation of the angular distribution of inelastically scattered electrons emitted from a negative-ion resonance of an oriented molecule. In this experiment, measured angular emission profiles for a physisorbed molecular O_2 overlayer adsorbed upon graphite were used to determine both the resonance symmetry and the structure of the overlayer.[1] In this paper we set out the new theoretical framework required to interpret these emission profiles and present the full details of our analysis of the O_2/graphite system.

The formation of temporary negative ions by low-energy electron impact upon atoms and molecules in the gas phase is a well-established phenomenon.[2,3] An electron which undergoes resonant scattering becomes temporarily trapped in a quasistable orbital localized within the target molecule, which decays to produce a characteristic angular distribution of emitted electrons. Recently there has been some interest in the prospects, and consequences, of the observation of resonances in molecules adsorbed upon solid surfaces. Whereas in the gas phase the molecules are rotationally disordered and the observed differential cross sections are a result of averaging over all possible molecular orientations, molecules physisorbed or chemisorbed upon a surface can be pinned in a fixed, albeit often unknown, orientation.

Davenport, Ho, and Schrieffer[4] have performed calculations of the angular distribution of electrons inelastically scattered from a number of oriented, isolated molecules. They obtained a series of angular profiles dependent upon the orientation of the molecular axis and realized that such results might be observed in high-resolution electron-energy-loss spectroscopy (HREELS) of adsorbed species; they proposed that these characteristic angular distributions might be used to determine the orientation of molecules at surfaces. Subsequently, Sanche and Michaud[5] and Demuth *et al.*[6] independently made the first observations of strong enhancements in the vibrational cross sections of certain diatomic molecules physisorbed upon polycrystalline metal films, demonstrating that negative-ion resonances can survive physisorption. Indeed, negative-ion resonances have now been observed in chemisorbed molecules, such as benzene on Pd(100) and Pd(111).[7]

In this paper we present detailed results of the first complete experimental study of the angular distribution of electrons inelastically scattered from a physisorbed molecular overlayer and develop a theoretical scheme by which these angular profiles can be interpreted in terms of both the molecular orientation and the nature of the negative-ion resonance. Preliminary results of this work have been presented elsewhere.[1]

II. RESONANT ELECTRON SCATTERING FROM ADSORBED SPECIES: BASIC PRINCIPLES

Any analysis of the angular distribution of electrons ejected from a negative-ion resonance must begin from an understanding of the emission from an isolated orientated molecule. Davenport and coworkers have predicted, in some detail, the characteristic features of resonant electron scattering from such molecules.[4] The key feature is that the incident electron "forgets" its initial direction when it becomes trapped in the resonant orbital and undergoes energy loss by stimulating a molecular vibration. This implies that the distribution of inelastically scattered electrons is purely determined by the symmetry of the quasibound orbital and orientation of the molecule. This is in strong contrast to the angular distribution of elastic scattering, which displays a characteristic forward-scattering peak arising from the requirement for the conservation of scattered particles.[8]

The differential cross sections for resonant electron scattering from an isolated molecule are obtained by matching the partial-wave expansion of the incoming and outgoing electron waves to the molecular–negative-ion state formed when the electron is trapped. The electron is ejected into the partial waves consistent with the sym-

metry of the resonant molecular orbital, which then dominate the angular distribution of scattered electrons. Similarly, the incident electrons tunnel into the resonant state via the same partial waves so that the differential *capture* cross section is the same as the differential cross section for electron emission.

When a molecule is adsorbed onto a surface, a number of other factors become important when compared to the isolated molecule. The surface breaks the molecular symmetry and modifies the resonance by mixing partial waves into the resonant orbital, which would otherwise be forbidden by the symmetry of the isolated molecule. For a shape resonance, the presence of additional partial waves having lower angular momentum allows the resonance to "leak" out through an effectively lower centrifugal barrier than in the gas phase. This is reflected in the energy and width of the resonance[9] and may also be expected to change the angular distribution of emitted electrons.

Another issue, which to date has received little attention, is the importance of elastic multiple scattering of the incident and ejected electrons among the surface atoms. When an electron is inelastically ejected from an adsorbed molecule, it can make its way to the detector along various paths. These paths may include scattering events which involve the substrate atoms and, in the case of a nondilute overlayer, the coabsorbed molecules. Similarly, electrons injected into the crystal from the electron gun may undergo elastic multiple scattering prior to forming a negative-ion resonance. We note, however, that the inelastic event breaks the coherence between the incoming and outgoing paths. It is well known that in the energy range within which resonances are typically observed (<20 eV), the elastic scattering cross section of an atom or molecule is similar to and often greater than its physical dimension. Indeed, all adequate descriptions of electron emission from surfaces within this energy range, such as for angle-resolved photoemission,[10] low-energy electron diffraction (LEED),[11–13] and impact scattering in HREELS (Refs. 14–16) take account of the strong elastic multiple scattering of electrons which occurs at these low energies. It is clear that a similar treatment will be needed in order to correctly interpret the detected angular distribution of inelastically scattered electrons emitted from a negative-ion resonance within a molecular overlayer.

III. THEORY OF ELECTRON EMISSION FROM NEGATIVE-ION RESONANCES AT SURFACES

A. Introduction

In this section we shall discuss the theory needed to calculate the angular distribution of inelastically scattered electrons emitted from a negative-ion resonance within a molecular overlayer. We shall focus upon the influence of elastic multiple scattering. The mechanism of electron capture, vibrational excitation of the molecule, and electron emission will be taken to behave as predicted by Davenport[4] and discussed earlier.

For a detected electron to have undergone energy loss it must have suffered an inelastic event at some point along its route from the electron gun to the detector. If the detector is tuned to collect electrons which have undergone an energy loss characteristic of resonant vibrational excitation, then the detected electrons must have participated in the formation of a molecular negative-ion resonance.

In order to calculate angular emission profiles we need to describe the interference of electron waves as they propagate through the surface. To do this we need to sum the multiple-scattering paths by which an electron is injected into the crystal by the electron gun, captured within a molecular–negative-ion resonance, and is then emitted from the resonant state to travel to the detector. Some of these paths are illustrated schematically in Fig. 1. We can split this process into three stages. First, we sum all *elastic* multiple-scattering paths by which an electron can arrive at the molecule. Next, we need to consider the capture of a proportion of these incident electrons within the molecular negative-ion resonance and their subsequent emission. Since the resonant state has a *differential* capture cross section, multiple scattering of the incident electrons will effect the extent to which the molecular resonance is excited. However, provided that a single partial wave dominates the capture and/or emission process, multiple scattering of the incident electrons does not influence the angular distribution of detected

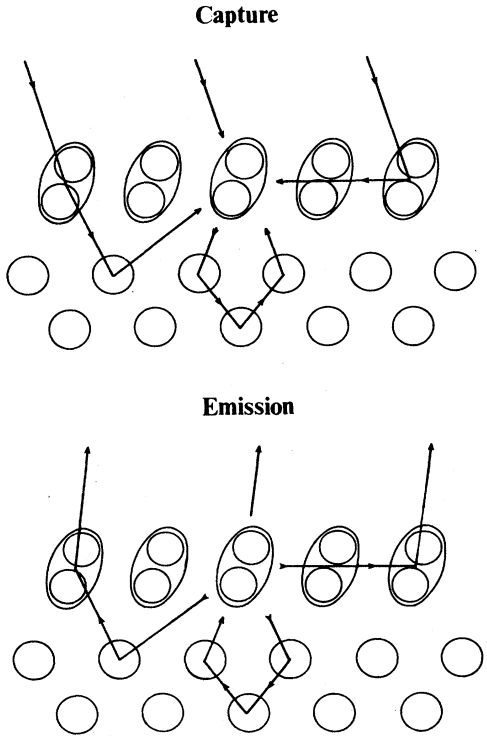

FIG. 1. A schematic illustration of some possible elastic multiple-scattering paths by which an electron propagates to (upper panel) and from (lower panel) a negative-ion resonance within a molecular overlayer. Each incident electron may undergo elastic and vibrational inelastic scattering from the same molecule by following a closed path such as the scattering loop illustrated in both panels.

electrons.[4] Finally, we need to sum all scattering paths by which these emitted electrons can be *elastically* multiply scattered by the overlayer molecules and substrate atoms to finally reach the detector. At this stage we consider each adsorbed molecule as an incoherent source of inelastically scattered electrons; in other words, electrons emitted from different molecules do not interfere.

At each stage we must consider scattering paths by which an electron returns to be scattered again by the molecule from which it was emitted or captured. The inclusion of these closed paths is crucial because in doing so we automatically include the process by which multiple scattering breaks the molecular symmetry and effectively mixes forbidden partial waves into the resonance. The importance of this effect in altering the resonant state has been predicted by the model calculations of Gerber and Herzenberg,[9] who also investigated the other mechanism responsible for symmetry breaking; the spatial *variation* of the image potential in the vicinity of the molecule. At present, we are unable to include the variation in the image potential in our theory since we employ a "muffin-tin" description of the atomic scattering, which requires a constant interstitial potential. Instead, we must model its effect by considering electron emission from appropriate perturbations of candidate gas-phase negative-ion resonances, as will be discussed later.

B. Formalism

Our main task is to evaluate the angular distribution of inelastically scattering electrons from an adsorbed molecular overlayer excited by an electron beam of energy E. For simplicity we shall assume that the surface consists of a substrate covered by a monolayer of a single molecular species in which the negative-ion resonance is excited, although the method can be generalized.

Consider the incident electron beam as a plane wave with momentum $\mathbf{k}_\parallel$ parallel to the surface,

$$\langle \mathbf{r}|\Phi_0^+(\mathbf{k}_\parallel,E)\rangle \equiv \exp(i\mathbf{K}_0^+\cdot\mathbf{r}) \ . \tag{1}$$

The incident electron wave vector $\mathbf{K}_0^+$ can be split into components parallel and perpendicular to the surface:

$$\mathbf{K}_0^+ = (\mathbf{k}_\parallel, K_{0z}^+) \ , \tag{2}$$

$$K_{0z}^+ = (K^2 - |\mathbf{k}_\parallel|^2)^{1/2} \ , \tag{3}$$

where $K=(2E-2V_0)^{1/2}$ is the magnitude of the electron wave vector within the surface corrected for the potential step V_0 at the interface. V_0 has an imaginary part, V_{0i}, which models the loss of electrons from the elastic scattering channel due to inelastic events.

If the surface occupies the half-space $z>0$, then the wave field of emitted electrons of energy $E-\alpha\delta E$ can be written as a set of plane waves leaving the surface:

$$\sum_{\mathbf{k}'_\parallel} D^\alpha(\mathbf{k}'_\parallel)\exp(i\mathbf{K}'\cdot\mathbf{r}), \quad z<0 \ . \tag{4}$$

Equation (4) describes the emission of inelastically scattered electrons which have excited a $0\rightarrow\alpha$ vibrational transition which has a fundamental energy loss of δE.

The corresponding detected intensity collected per unit solid angle is[17]

$$I^\alpha(\theta,\phi) = |D^\alpha(\mathbf{k}'_\parallel)|^2 N_m K^2 \Omega \cos^2\theta / |K_{0z}^+| \ , \tag{5}$$

where (θ,ϕ) are the polar and azimuthal angles of emergence corresponding to $\mathbf{k}'_\parallel$, and N_m the number of molecules in the area of the surface, Ω, illuminated by the incident electron beam.

The amplitude of inelastically scattered plane waves, $D^\alpha(\mathbf{k}'_\parallel)$, can be written as a matrix element between two "LEED states,"

$$D^\alpha(\mathbf{k}'_\parallel) = (iK/4\pi)\langle \Phi(\mathbf{k}'_\parallel, E-\alpha\,\delta E)|f^{\alpha 0}|\Phi(\mathbf{k}'_\parallel,E)\rangle \ , \tag{6}$$

where $\langle \mathbf{r}|\Phi(\mathbf{k}'_\parallel,E)\rangle$ is the wave function produced by an incident electron beam with parallel momentum $\mathbf{k}_\parallel$ and energy E being elastically multiply scattered by the atoms and molecules of the surface. $f^{\alpha 0}$ describes how two such LEED states are coupled together by a $0\rightarrow\alpha$ vibrational excitation of a single molecule.[18] The total detected intensity expressed in Eq. (5) is an incoherent sum of the wave field emitted from each excited molecule.

Similar matrix elements to that of Eq. (6) may be found in related electron-emission problems such as photoemission,[10] LEED,[19,20] and impact scattering in HREELS.[14–16] Therefore, since a full explanation of this equation may be found in these references, the derivation of Eq. (6) will not detain us here. What will concern us, in the case of resonant scattering, is the form of f which describes the capture, vibrational excitation, and emission arising from a negative-ion resonance of one molecule within the overlayer.

Let us switch to an angular momentum basis and insert two complete sets of states into Eq. (6):

$$D^\alpha(\mathbf{k}'_\parallel) = (iK/4\pi) \times \sum_{(l,m)(l',m')} \langle \Phi(\mathbf{k}'_\parallel, E-\alpha\,\delta E)|l'm'\rangle \times \langle l'm'|f^{\alpha 0}|lm\rangle\langle lm|\Phi(\mathbf{k}_\parallel,E)\rangle \ . \tag{7}$$

$\langle \mathbf{r}|lm\rangle$ is a spherical harmonic defined in the molecular frame,

$$\langle \mathbf{r}|lm\rangle = Y_{lm}(\mathbf{r}) \ . \tag{8}$$

$\langle l'm'|f^{\alpha 0}|lm\rangle \equiv f^{\alpha 0}_{l'm',lm}$ is the transition amplitude for inelastic resonant scattering by the molecule, as defined by Davenport and co-workers.[4] $f^{\alpha 0}_{l'm',lm}$ is the probability amplitude for an electron to tunnel into the molecular resonance through the partial wave (l,m) and then to decay into the partial wave (l',m'), having undergone a $0\rightarrow\alpha$ vibrational loss.

To proceed further we need to calculate the amplitudes $\langle lm|\Phi(\mathbf{k}_\parallel,E)\rangle$. In the vicinity of an excited molecule, the LEED wave function $\langle \mathbf{r}|\Phi(\mathbf{k}_\parallel,E)\rangle$ can be expanded in spherical waves about the center of mass of the molecule. Assuming, for simplicity, that this point is the origin, then

$$\langle \mathbf{r}|\Phi(\mathbf{k}_\parallel,E)\rangle = \sum_{l,m} A_{lm}(\mathbf{k}_\parallel,E) j_l(Kr) Y_{lm}(\mathbf{r}) + \sum_{l,m}\left[\sum_{l',m'} A_{l'm'}(\mathbf{k}_\parallel,E) f^{00}_{l'm',lm}\right] \times h_l^1(Kr) Y_{lm}(\mathbf{r}) , \quad (9)$$

and similarly for $\langle \mathbf{r}|\Phi(\mathbf{k}'_\parallel,E-\alpha dE)\rangle$. j_l is a spherical Bessel function and h_l^1 a Hankel function of the first kind. $f^{00}_{l'm',lm}$ is the *elastic* scattering T matrix of the molecule; terms containing $f^{\alpha 0}_{l'm',lm}$ for $\alpha \neq 0$ do not appear, since $\langle \mathbf{r}|\Phi(\mathbf{k}_\parallel,E)\rangle$ is the wave function for *elastic* scattering. It follows from Eq. (9) that

$$A_{l,m}(\mathbf{k}_\parallel,E) \equiv \langle lm|\Phi(\mathbf{k}_\parallel,E)\rangle . \quad (10)$$

The remaining amplitude on the left-hand side of Eq. (8) is obtained by exploiting the reciprocity theorem,[21-23] which gives

$$\langle \Phi(\mathbf{k}'_\parallel,E-\alpha\delta E)|lm\rangle = [(-1)^m/2i|k'_z|\Omega K] \times \langle l-m|\Phi(\mathbf{k}'_\parallel,E-\alpha\delta E)\rangle . \quad (11)$$

Substituting Eqs. (11) and (10) into (8) we find

$$D^\alpha(\mathbf{k}_\parallel) = (8\pi\Omega|k'_z|)^{-1} \times \sum_{(l',m'),(l,m)} (-1)^{m'} A_{l'-m'}(\mathbf{k}'_\parallel,E-\alpha\delta E) \times f^{\alpha 0}_{l'm',lm} A_{lm}(\mathbf{k}_\parallel,E) , \quad (12)$$

where $A_{lm}(\mathbf{k}_\parallel,E)$ is seen to be the amplitude of spherical waves in the molecular frame incident upon the excited molecule due to the elastic multiple scattering of an incident electron beam of energy E and parallel wave vector $\mathbf{k}_\parallel$. In essence, Eq. (12) describes the coupling of a "normal" LEED state for an incident beam with parallel wave vector $\mathbf{k}_\parallel$ and a "time-reversed" LEED state of opposite wave vector to that of the detected electrons, $\mathbf{k}'_\parallel$. To calculate the spherical-wave amplitudes A_{lm} we can employ conventional LEED methods.[11-13] In fact, these amplitudes can be obtained directly from a standard LEED calculation suitably modified to treat a molecular overlayer.

If there were no elastic multiple scattering, then an incident electron beam would arrive unperturbed at the molecule. The LEED wave function $\langle \mathbf{r}|\Phi(\mathbf{k}_\parallel,E)\rangle$ would then be a single plane wave of parallel momentum $\mathbf{k}_\parallel$ and energy E;

$$\langle \mathbf{r}|\Phi(\mathbf{k}_\parallel,E)\rangle = \exp(i\mathbf{K}_0^+\cdot\mathbf{r}) , \quad (13)$$

in which case

$$\langle lm|\Phi(\mathbf{k}_\parallel,E)\rangle \equiv A_{lm}(\mathbf{k}_\parallel,E) = 4\pi i^l Y^*_{lm}(\mathbf{K}_0^+) . \quad (14)$$

Substituting Eq. (14) into (12) we obtain the angular distribution of inelastically scattered electrons with energy $E-\alpha\delta E$:

$$I^\alpha(\theta,\phi) = n_m \left| \sum_{(l',m'),(l,m)} i^{(l-l')} Y_{l'm'}(\mathbf{K}') \times f^{\alpha 0}_{l'm',lm} Y^*_{lm}(\mathbf{K}_0^+) \right|^2 , \quad (15)$$

where n_m is the number of activated molecules per unit surface area. Equation (15) is equivalent to Davenport's expression for the differential cross section for scattering from an isolated oriented molecule.[4] However, as we shall show in the next section, such a simple picture is inadequate and full multiple-scattering corrections to Eq. (14) must be included.

It remains to evaluate the transition amplitude $f^{\alpha 0}_{l'm',lm}$. Both Davenport and co-workers and Gerber and Herzenberg have shown how to do this, either starting from a $X\alpha$ scattered-wave ($X\alpha$-SW) calculation of the molecular electronic structure[4] or from previously calculated eigenphase sums.[9] However, it is not necessary to go to these lengths in the case where a single partial wave dominates the capture and emission from the resonance. Thus, for example, in the case of a $^4\Sigma_u$ resonance in O_2 the $p\sigma$ partial wave is expected to dominate the capture and emission process, so that Eq. (12) becomes

$$D^\alpha(\mathbf{k}_\parallel) = A_{10}(\mathbf{k}'_\parallel,E-\alpha\, dE) f^{\alpha 0}_{10,10} A_{10}(\mathbf{k}_\parallel,E) , \quad (16)$$

and in the no-scattering limit:

$$I^\alpha(\theta,\phi) = n_m |f^{\alpha 0}_{10,10}|^2 \cos^2(\theta_i-\theta_m)\cos^2(\theta-\theta_m) , \quad (17)$$

where θ_m is the polar angle between the molecular axis and the surface normal and θ_i the polar angle of incident. Thus, we obtain the $\cos^2$ angular distribution of inelastically scattered electrons which is characteristic of pure p-wave emission.

IV. APPLICATION TO PHYSISORBED O_2 ON GRAPHITE

In this section we shall use the theoretical framework developed in the previous section to interpret measured angular emission profiles from a model molecular overlayer system; the $\zeta 2$ phase of O_2 on graphite.

The $\zeta 2$ phase of O_2 on graphite has been characterized by several diffraction studies.[24-27] This phase exists at temperatures between 18 and 38 K (Ref. 28) and has a hexagonal unit cell with a lattice parameter of 3.30 ± 0.03 Å. Prior to the present study, the molecular orientation within the overlayer was unknown, but the layer lattice constants compared to the size of the O_2 molecule have been taken to imply that the molecule stands upright on the surface. However, it has been pointed out that there is sufficient room for the molecules to tilt slightly towards the surface.[26] The details of this experiment and the method of preparation of the $\zeta 2$ phase have been fully described elsewhere[1] but for completeness are summarized here.

By monitoring the intensity of the ($\nu=0\rightarrow1$) vibrational loss peak in the electron-energy-loss spectrum as a function of the incident beam energy, we have observed a broad resonance in the vibrational scattering cross sec-

tion with a peak between 8.5 and 9 eV in O_2 on graphite.[1] The observed sequence of vibrational overtones has a fundamental frequency of 191±3 meV, which is close to the gas-phase O—O stretch frequency of 194 meV,[29] indicating that we are observing a molecular negative-ion resonance of physisorbed O_2. A number of gas-phase negative-ion resonances have been observed from O_2 below 20 eV,[3] but on energy grounds there are only two contenders for the observed vibrational excitation in the 6–11-eV energy range.[1,30,31] In fact, a similar broad profile, with a peak close to 9.5 eV, has been observed in the gas phase and attributed to a $^4\Sigma_u$ shape resonance.[29] However, we should be aware that in the gas phase there also exists a broad $^2\Pi_u$ Feshbach resonance, which is believed to give rise to dissociative attachment close to 7 eV in both the gas phase and condensed O_2.[3,32]

The angular distributions of emitted electrons corresponding to this observed negative-ion resonance were measured by monitoring the intensity of the $v=0\rightarrow 1$ loss peak,[33] as a function of the polar emission angle for an incident electron energy of 8.5 eV. The type of graphite used was highly oriented pyrolytic graphite (HOPG) (Ref. 33), so that the measured angular profile is an average over the complete azimuthal range of domain orientations present on this surface.

In the remainder of this paper we wish to answer two fundamental questions. First, what is the nature of the negative-ion resonance which produces the observed resonant scattering from O_2 on graphite? In particular, we wish to know the symmetry of the resonance and how it differs, if at all, from the corresponding gas-phase resonances. Secondly, can these angular profiles be used to determine the orientation of the molecular axis within the O_2 monolayer?

In order to attempt to answer these questions we have constructed a calculational scheme based upon the multiple-scattering theory described in the previous section. The core of this calculation is the evaluation of the LEED states of Eq. (6) which was achieved by adapting an existing suite of LEED computer codes. In such programs, which are described in considerable detail elsewhere,[11–13] the surface is usually taken to be composed of a stack of layers of atoms. The crystal potential is modeled by a lattice of muffin-tin potentials, each characterized by a set of phase shifts. Electron energies are measured relative to the muffin-tin zero and are corrected for the step in potential at the surface barrier. The incident electron wave function within the surface is described in a mixed basis. Between the atomic planes the electron wave field consists of a set of plane waves (beams), each characterized by its momentum parallel to the surface. Intralayer scattering is performed in an angular momentum basis, in which the electron wave field consists of a set of spherical partial waves.

In most conventional LEED calculations, a molecular overlayer would usually be constructed from several planes of its constituent atoms. However, in the case of resonant scattering, it is necessary to consider the molecule as a whole and first construct a molecular scattering potential, which we have incorporated into the conventional LEED scheme as a single plane of *molecules*. We have implemented the multiple-scattering method (MSM) of Dill and Dehmer[34] to evaluate the elastic scattering T matrix of the O_2 molecule. In the absence of a full self-consistent-field molecular-orbital (SCF-MO) calculation, we have followed the original prescription of these authors and utilized a superposition of Roothan-Hartree-Fock atomic O_2 wave functions tabulated by Clementi and Roetti.[35] Although we do not regard such a simple scheme as an adequate treatment of elastic scattering at very low energies (i.e., $\lesssim 2$ eV), we have found it acceptable at least for energies above 8 eV.

As a test of the accuracy of this molecular calculation we evaluated the total and partial elastic scattering cross sections shown in Fig. 2. By evaluating the eigenphase sums[36] of the molecular T matrix we identify a $^4\Sigma_u$ *elastic* resonance at 11.75 eV, giving a peak in the total cross section of 10.7 Å^2. The values may be compared with the measured gas-phase values of approximately 11 eV and 9.5 Å^2, respectively.[37] Clearly, the agreement is quite satisfactory and therefore we believe that our description of the elastic scattering by the O_2 molecule at 8.5 eV is sufficiently accurate for the purposes of this paper.

The calculated O_2 differential cross sections were inserted into our calculational scheme to generate the spherical-wave amplitudes A_{lm} of Eq. (12). The effective reflectivity of the graphite substrate was calculated to be less than 1% at 8.5±0.5 eV, and therefore, since the $\zeta 2$ phase of O_2 is incommensurate, multiple-scattering paths within the graphite, which have a minimal effect upon the calculated emission profiles, were neglected.[1] To describe the intraplanar elastic scattering we used l values from 0 to 5 requiring six phase shifts for each atomic

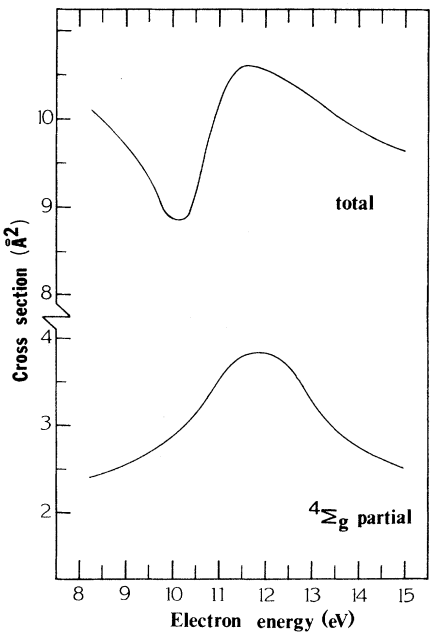

FIG. 2. Calculated elastic scattering cross section of O_2 as a function of incident electron energy, demonstrating the existence of a $^4\Sigma_u$ elastic shape resonance at 11.75 eV.

species. To describe the inelastic damping of elastic scattering, the imaginary part of the constant potential within the surface was set to -2 eV. This value of V_{0i} was chosen so that the widths of features in the calculated angular profile were comparable to those observed. Lower values, $-0.5 \leq V_{0i} \leq 2.0$ eV, introduce more fine structure and give slightly sharper peaks, albeit at the same position relative to the surface normal.

In order to illustrate the importance of multiple scattering we display in Fig. 3 the calculated angular distribution of inelastically scattered electrons ejected along the [11] direction in **k** space from a *single* domain of O_2 on graphite. The electron beam is incident at an angle of 65° to the normal in the same plane as the [11] direction of the O_2 monolayer, in which the molecules are chosen to tilt by 25° from the normal. The profiles shown in Fig. 3 were calculated assuming resonant emission and for capture into three different partial waves. The $p\sigma$ and $p\pi$ partial waves correspond to the formation of pure $^4\Sigma_u$ or $^2\Pi_u$ negative-ion resonances, respectively. The *s*-wave profile might be expected if the molecular inversion symmetry were strongly broken upon physisorption. In this case an "*s*" partial wave could be mixed into a $^4\Sigma_u$ resonance and might provide the dominant decay or capture channel for the trapped electron. For comparison we also show the corresponding no-scattering profiles, in which the detected intensities become simple $\cos^2$, $\sin^2$, or constant ($=1$) distributions.

From Fig. 3 we can immediately see that multiple scattering plays an important role in determining the angular profiles at 8.5 eV. Indeed, for some profiles the intensity is enhanced by a factor of 2 or 3 at some emission angles. We see a sharpening of peaks in **k** space and additional structure which is not present in the no-scattering profiles—general trends which have also been observed in other electron-emission profiles, such as those seen in angle-resolved photoemission.[10] We note that multiple scattering has a particularly important influence upon the $p\pi$ profile, where electrons are predominantly ejected directly into the plane of the O_2 monolayer. In contrast, the angular distribution of electrons emitted into the $p\sigma$ partial wave remains relatively unperturbed, since electrons are initially ejected predominantly out of the plane of the overlayer. However, Fig. 3 serves to emphasize that in order to interpret measured resonant profiles we need a proper method of calculating the angular distributions, which includes full multiple scattering.

In Fig. 4 we display a series of calculated angular profiles for a range of molecular tilt angles for $p\sigma$-, $p\pi$-, and *s*-wave emission. These angular distributions were calculated for an overlayer in which the molecules tilt into the "gap" between two of the adjacent O_2 molecules (i.e., the [11] direction of the hexagonal O_2 overlayer). Unlike the profiles shown in Fig. 3, which were for a sin-

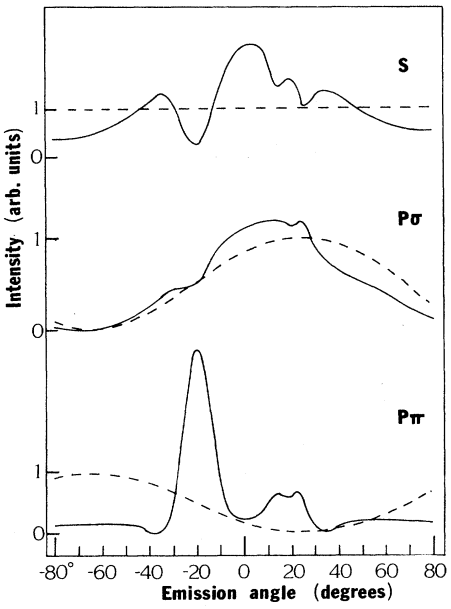

FIG. 3. Calculated angular distribution of $v=0 \rightarrow 1$ loss intensity for a single domain of the $E2$ phase of O_2 on graphite in which the molecular tilt angle is 25°. Profiles are shown for emission into *s* (upper curves), $p\sigma$ (central curves), and $p\pi$ (lower curves) partial waves for full multiple scattering (solid curves) and in the no-scattering limit (dashed curves). The detector, electron gun, and tilted molecule all lie within the [11] direction of the hexagonal overlayer.

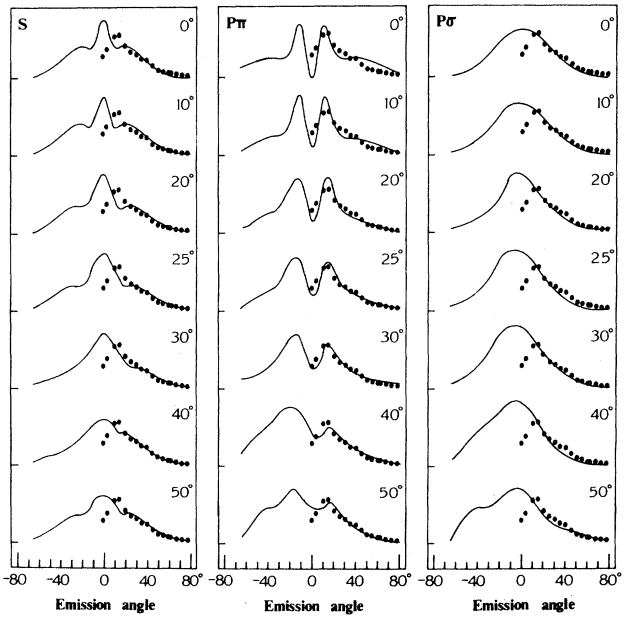

FIG. 4. Comparison of calculated (solid curves) and measured (solid circles) angular emission profiles for physisorbed O_2 on HOPG. The incident electrons impinge upon the surface at an angle of 65° to the surface normal with an energy of 8.5 eV. Calculated profiles are shown for molecular tilt angles of between 0° and 50° for emission and capture via *s*, $p\pi$, and $p\sigma$ partial waves. Each pair of curves has been normalized by equating the area under each profile and the calculated angular distributions have been convoluted by the detector response function, which has a width of 2.5°.

gle domain, the profiles of Fig. 4 have been azimuthally averaged over the complete azimuthal range of domain orientations present on HOPG and therefore may be directly compared with experiment. One result of this azimuthal averaging is that the calculated distributions are largely insensitive to the direction of tilt of the O_2 molecules, at least for small tilt angles $\leq 30°$. Therefore we are unable to distinguish between various tilt directions on the surface and limit our discussion to the overlayer structure described above. By comparing the calculated angular profiles and the superimposed measured angular distributions we are able to both identify the nature of the resonant state and determine the orientation of the O_2 molecule within the overlayer.

Let us first attempt to identify the resonant-state symmetry. From Fig. 4 we see that we can exclude emission into a $p\sigma$ partial wave as the source of the detected electrons. The calculated profiles for this resonance have a single broad peak which lies on the other side of the surface normal to that of the measured distribution, and there is no evidence for the observed dip in intensity near the surface normal—whatever the molecular tilt. Similarly, we can exclude emission into a pure s wave. However, the emission and capture via a $p\pi$ partial wave does give rise to calculated angular profiles which resemble those measured. For a range of the molecular orientations considered, the characteristic features of the experimental profile are reproduced, notably the dip in intensity near the surface normal and the single peak close to 15°. In particular, for molecular tilt angles between 20° and 30° we obtain highly satisfactory visual agreement.

A more quantitative estimate of the molecular tilt angle can be made by an appropriate numerical comparison of the experimental and calculated profiles. To do this we utilize a reliability (R) factor which is routinely employed in LEED I/V analysis.[13] We have chosen to use the R factor R_{RPI}, which is particularly sensitive to the location of intensity extreme while being insensitive to the presence of any background contribution and the relative intensity scales of the measured and calculated profiles. R_{RPI} is defined as a function of the derivative of the emitted intensity with respect to the polar emission angle θ, $I'(\theta)$:[13]

$$R_{\mathrm{RPI}} = A \int [I'_{\mathrm{expt}}(\theta) - cI'_{\mathrm{theor}}(\theta)]^2 \, d\theta \, , \tag{18}$$

where

$$A = 1 \Big/ \int [I'_{\mathrm{expt}}(\theta)]^2 \, d\theta \, , \tag{19}$$

c normalizes the experimental and calculated angular distributions to each other, and the integral is over all detection angles. Clearly, the smaller the value of R_{RPI} the better the theory-experiment fit; $R_{\mathrm{RPI}} = 0$ denotes perfect agreement.

In Fig. 5 we display the R-factor comparison of calculated and measured emission profiles for angles of incidence of 50° and 65° (shown in Fig. 4). From Fig. 5 it is clear that for *both angles of incidence* $p\pi$ emission and capture provides the best fit to experiment, for which

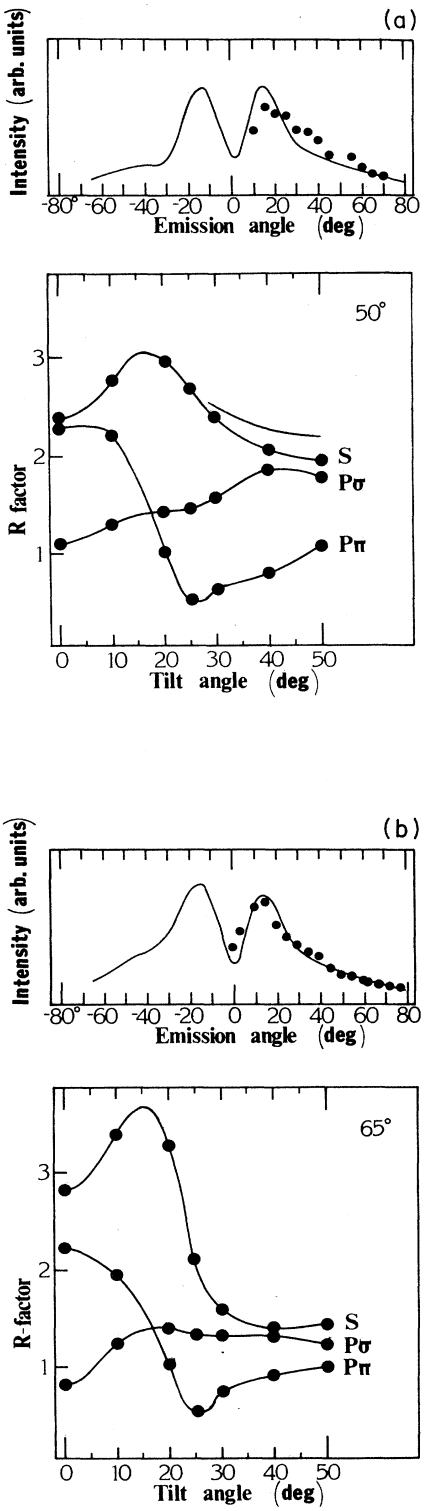

FIG. 5. R-factor comparison of the O_2/graphite calculated and measured emission profiles for capture and emission via s, $p\pi$, and $p\sigma$ partial waves for incident beam angles of 50° and 65°. For both angles of incidence the R-factor minimum ($R_{\mathrm{RPI}} = 0.50$) occurs for a molecular tilt angle of 25° for the $p\pi$ partial wave. The comparison of the best-fit calculated and observed profiles is shown in the upper panels.

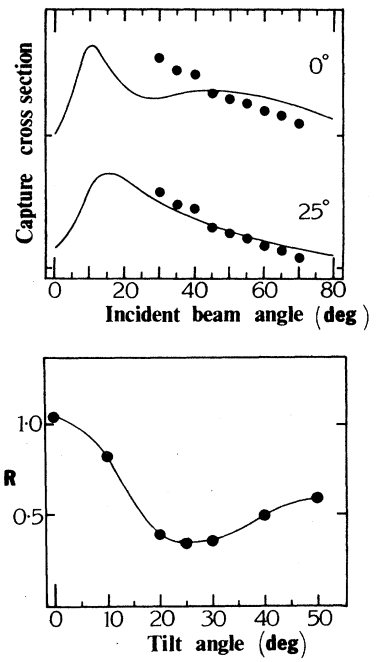

FIG. 6. R-factor comparison of O_2/graphite and the calculated and observed effective capture cross sections at an emission angle of 32.5°, assuming capture and emission via a $p\pi$ partial wave. The R-factor minimum occurs for a molecular tilt angle of 25°.

there is a strong minimum at a molecular tilt angle of 25°. Thus we conclude that only emission and/or capture via a $p\pi$ partial wave can account for the observed angular distributions. This result is consistent with the observation of the $^2\Pi_u$ negative-ion resonance but not the $^4\Sigma_u$ state.

Our conclusions are confirmed by Fig. 6, which shows the capture cross section of the observed negative-ion resonance. The experimental profile was obtained by monitoring the intensity of the $v=0\rightarrow 1$ loss peak in the electron-energy-loss spectrum as a function of the incident beam angle at a fixed angle of 32.5° to the surface normal. The calculated capture cross section is compared to the measured quantity by the R factor of Eq. (18). Although geometrical constraints restricted the angular range over which the capture cross section could be measured, it is clear that $p\pi$ emission and capture provides a satisfactory fit to experimental data for a molecular tilt angle of around 25°, in agreement with the result derived from the emission profiles.

In addition to the profiles shown in Figs. 4 and 6, we also considered "perturbations" of the $^4\Sigma_u$ and $^2\Pi_u$ resonant states, in which capture and emission takes place through different partial waves such as "s-in,p-out" and "p-in,s-out".[4] None of these profiles resembled those measured for any molecular tilt angle. We have also investigated the influence of variations in several structural and nonstructural parameters of the surface. We made changes in the lattice parameters of the O_2 overlayer consistent with the accuracy (±0.03 Å) of the previous LEED determination of the structure of the $\zeta 2$ phase. These variations had little influence upon the calculated profiles and do not change our assignment of the resonance symmetry or the molecular tilt angle.

We conclude that only emission and capture via a $p\pi$ partial wave can account for the observed angular distributions from O_2 physisorbed on graphite. This implies that the $^2\Pi_u$ negative-ion state[38] makes the dominant contribution to the observed resonant scattering at 8.5±0.5 eV and that the O_2 molecular axis stands at 25° from the surface normal in what we believe to be the $\zeta 2$ phase. On the basis of the visual comparison shown in Fig. 4 and the R-factor analysis in Fig. 5, we estimate that the error in our assignment of the molecular tilt angle to be approximately ±5°.

V. CONCLUSIONS

In this paper we have presented a theoretical method for calculating resonance-scattering angular distributions from adsorbed species. We have demonstrated, by application to experimental data obtained for physisorbed O_2 on graphite, that this method can be used to determine both the partial-wave content of the temporary negative ion and the orientation of the molecular axis within the overlayer. The crucial ingredient in this theory is a proper treatment of the multiple scattering of the incident and emitted electrons and we expect these strong dynamical effects to play an important role in determining the angular emission profiles in the entire energy range within much negative ion resonances are observed.

The calculational method developed in this paper is quite general, provided that the approximations employed in the LEED methods upon which our theory is based remain valid. The limitations of conventional LEED theory are discussed elsewhere[13] but probably rule out the application of the methods presented here to resonance scattering at energies substantially below 10 eV (e.g., the 0–2-eV energy range[6]).

ACKNOWLEDGMENTS

We are most grateful to J. L. Wilkes for his help with the experimental work. We wish to acknowledge the United Kingdom Science and Engineering Research Council for financial support for this work and for the allocation of computational resources on the Cray X-MP located at the Rutherford-Appleton Laboratory, U.K. R.E.P. thanks the Royal Commission for the Exhibition of 1851 for continued support.

[1]R. E. Palmer, P. J. Rous, J. L. Wilkes, and R. F. Willis, Phys. Rev. Lett. **60**, 329 (1988).
[2]George J. Schulz, Rev. Mod. Phys. **45**, 378 (1973).
[3]George J. Schulz, Rev. Mod. Phys. **45**, 423 (1973).
[4]J. W. Davenport, W. Ho, and J. R. Schrieffer, Phys. Rev. B **17**, 3115 (1978).
[5]L. Sanche and M. Michaud, Phys. Rev. Lett. **47**, 1008 (1981).
[6]J. E. Demuth, D. Schmeisser, and Ph. Avouris, Phys. Rev.

Lett. **47**, 1166 (1981).
[7]See, for example, L. L. Kesmodel, Phys. Rev. Lett. **53**, 1001 (1984); G. D. Waddill and L. L. Kesmodel, Phys. Rev. B **32**, 2107 (1985).
[8]L. I. Schiff, *Quantum Mechanics* (McGraw-Hill, New York, 1981), pp. 137 and 138.
[9]A. Gerber and A. Herzenberg, Phys. Rev. B **31**, 6219 (1985).
[10]J. B. Pendry and A. Liebsh, in *Photoemission and Electronic Properties of Surfaces,* edited by B. Feuerbacher, B. Fitton, and R. F. Willis (Wiley, New York, 1978), Chap. 4 and 7.
[11]J. B. Pendry, *Low Energy Electron Diffraction* (Academic, New York, 1974).
[12]M. A. Van Hove and S. Y. Tong, *Surface Crystallography by LEED* (Springer, Berlin, 1979).
[13]M. A. Van Hove, W. H. Weinberg, and C.-M. Chan, *Low Energy Electron Diffraction* (Springer, Berlin, 1986).
[14]G. C. Aers and J. B. Pendry, Comput. Phys. Commun. **25**, 389 (1982).
[15]S. Y. Tong, C. H. Li, and D. L. Mills, Phys. Rev. Lett. **44**, 407 (1980).
[16]T. B. Grimley and K. L. Sebastian, J. Phys. C **3**, 5645 (1980).
[17]J. B. Pendry, J. Phys. C **8**, 2415 (1975).
[18]We have included the prefactor of $iK/4\pi$ in Eq. (6) so as to be simultaneously consistent with Davenport's definition of the transition amplitude f (see Ref. 6) and the usual normalization of the LEED states (see Ref. 13).
[19]P. J. Rous, J. B. Pendry, D. K. Saldin, K. Heinz, K. Muller, and N. Bickel, Phys. Rev. Lett. **57**, 2951 (1986).
[20]P. J. Rous and J. B. Pendry, Comput. Phys. Commun. (to be published).
[21]D. P. Woodruff and B. W. Holland, Phys. Lett. **31A**, 207 (1970).
[22]D. E. Bilhorn, L. L. Foldy, R. M. Thaler, W. Tobocman, and V. A. Madsen, J. Math. Phys. **5**, 435 (1964).
[23]A. P. Pogany and P. S. Turner, Acta Crystallogr. Sect. A **24**, 103 (1968).
[24]D. D. Awschalom, G. N. Lewis, and S. Gregory, Phys. Rev. Lett. **51**, 586 (1983).
[25]J. P. McTague and M. Nielsen, Phys. Rev. Lett. **37**, 596 (1976); M. Nielsen and J. P. McTague, Phys. Rev. B **19**, 3096 (1979).
[26]Michael F. Toney and Samuel C. Fain, Jr., Phys. Rev. B **30**, 1115 (1984).
[27]P. W. Stephens, P. A. Heiney, R. J. Birgeneau, P. M. Horn, J. Stoltenberg, and O. E. Vilches, Phys. Rev. Lett. **45**, 1959 (1980); P. A. Heiney, P. W. Stephens, S. G. J. Mochrie, J. Akimitsu, R. J. Birgeneau, and P. M. Horn, Surf. Sci. **125**, 539 (1983); S. G. J. Mochrie, M. Sutton, J. Akimitsu, R. J. Birgeneau, P. M. Horn, P. Dimon, and D. E. Moncton, *ibid.* **138**, 599 (1984).
[28]Hoydoo You and Samuel C. Fain, Jr., Phys. Rev. B **33**, 5886 (1983).
[29]P. H. Krupenie, J. Phys. Chem. Ref. Data. **1**, 423 (1972).
[30]R. Azria, L. Parenteau, and L. Sanche, Phys. Rev. Lett. **59**, 638 (1987).
[31]S. F. Wong, M. J. W. Boness, and G. J. Schulz, Phys. Rev. Lett. **31**, 969 (1973).
[32]L. Sanche, Phys. Rev. Lett. **53**, 1638 (1984).
[33]M. S. Dresselhaus and G. Dresselhaus, Adv. Phys. **30**, 139 (1981).
[34]D. Dill and J. L. Dehmer, J. Chem. Phys. **61**, 692 (1974).
[35]E. Clementi and C. Roetti, *Atomic Data and Nuclear Data Tables* (Academic, New York, 1974).
[36]J. L. Dehmer and D. Dill, J. Chem. Phys. **65**, 5327 (1976).
[37]Loucas G. Christophorous, J. Phys. Chem. **12**, 19 (1978); S. Trajmar, D. C. Cartwright, and W. Williams, Phys. Rev. A **4**, 1482 (1971).
[38]R. E. Palmer, P. J. Rous, and R. F. Willis, in *Proceedings of the Satellite Meeting to the XV International Conference on the Physics of Electronic at Atomic Collisions: Electron Molecule Scattering and Photoionization, Daresbury, 1987,* edited by P. G. Burke and J. B. West (Plenum, New York, in press).